

# Cotyledon cells of *Vigna mungo* seedlings use at least two distinct autophagic machineries for degradation of starch granules and cellular components

Kiminori Toyooka,<sup>1,2</sup> Takashi Okamoto,<sup>1</sup> and Takao Minamikawa<sup>1</sup>

<sup>1</sup>Department of Biological Sciences, Tokyo Metropolitan University, Tokyo, 192-0397 Japan

<sup>2</sup>Department of Infectious Diseases and Tropical Medicine, International Medical Center of Japan, Tokyo, 162-8655 Japan

$\alpha$ -Amylase is expressed in cotyledons of germinated *Vigna mungo* seeds and is responsible for the degradation of starch that is stored in the starch granule (SG). Immunocytochemical analysis of the cotyledon cells with anti- $\alpha$ -amylase antibody showed that  $\alpha$ -amylase is transported to protein storage vacuole (PSV) and lytic vacuole (LV), which is converted from PSV by hydrolysis of storage proteins. To observe the insertion/degradation processes of SG into/in the inside of vacuoles, ultrastructural analyses of the cotyledon cells were conducted. The results revealed that SG is inserted into LV through autophagic function of LV and subsequently degraded by vacuolar  $\alpha$ -amylase. The autophagy for SG was structurally similar to micropexoph-

agy detected in yeast cells. In addition to the autophagic process for SG, autophagosome-mediated autophagy for cytoplasm and mitochondria was detected in the cotyledon cells. When the embryo axes were removed from seeds and the detached cotyledons were incubated, the autophagosome-mediated autophagy was observed, but the autophagic process for the degradation of SG was not detected, suggesting that these two autophagic processes were mediated by different cellular mechanisms. The two distinct autophagic processes were thought to be involved in the breakdown of SG and cell components in the cells of germinated cotyledon.

## Introduction

Seeds of higher plants accumulate storage materials such as carbohydrates and proteins in cotyledons or endosperms, and the reserves are degraded to supply carbon and nitrogen sources to further seedling growth (Bewley and Black, 1994). Endospermic monocotyledon seeds store the reserves in the endosperms, which are derived from the fertilization of a central cell in the ovule with a sperm cell from the pollen grains (for review see Russell, 1992). After or during the deposition of the reserves, cells in the endosperm die through possible programmed cell death, which is induced by ethylene, a plant hormone (Young et al., 1997). When the monocotyledon seeds are germinated, the reserves in the endosperms are degraded by hydrolases that are secreted from aleurone layers (for reviews see Akazawa and Hara-Nishimura, 1985; Fincher, 1989). In other words, endosperms in germinated cereal grains are sites of a mixture of

storage materials and hydrolases, such as amylases and proteases, which are synthesized de novo in aleurone layers by the induction of gibberellic acids (Baulcombe and Buffard, 1983; Jacobsen and Beach, 1985; Koehler and Ho, 1990; Shintani et al., 1997; Sutoh et al., 1999).

In contrast to monocot seeds, many nonendospermic dicotyledon seeds store the reserves in cotyledon cells, which are developed from the fusion of an egg cell with a sperm cell (for review see Russell, 1992), and the cotyledon cells are still alive even when the seeds germinate. In addition, the pattern of the degradation of storage materials in the cotyledons is well ordered. In cotyledons of kidney bean and mung bean seedlings, the mobilization of reserves is initiated in the cells positioned furthest from the vascular bundle (VB),\* and the degradation progresses toward the VB according to the progress of germination. On the other hand, the use of reserves first occurs in the cells nearest to the VB, and the breakdown progresses to the outer cotyledon cells in soybean and favabean seedlings (Bewley and Black, 1978).

Address correspondence to Dr. Takashi Okamoto, Department of Biological Sciences, Tokyo Metropolitan University, Minami-osawa, Hachioji, Tokyo, 192-0397 Japan. Tel.: 81-426-77-2562. Fax: 81-426-77-2559. E-mail: okamoto-takashi@c.metro-u.ac.jp

Key words:  $\alpha$ -amylase; autophagy; intracellular transport; vacuole; senescence

\*Abbreviations used in this paper: KV, KDEL-tailed cysteine proteinase-accumulating vesicle; LED, low electron density; LV, lytic vacuole; PSV, protein storage vacuole; SG, starch granule, VB, vascular bundle.

Such well-ordered degradation processes have been explained by the programmed cell death of plants (Greenberg, 1996; Pennell and Lamb, 1997). Senescence of higher plants is the final phase of a plant organ's development, involves the active turnover and recapture of cellular materials for use in other organs (Nooden, 1988), and requires nuclear functions, suggesting it is an active and programmed process (Ness and Woolhouse, 1980). Cotyledons of dicotyledon seeds are leaves specialized for storage of reserves, and they change to senescence organs from vegetative organs at the stage of seed germination and subsequent seedling growth.

In cotyledons of *Vigna mungo* seeds, proteins and starch are stored in protein storage vacuoles (PSVs) and starch granules (SGs), respectively (Harris and Chrispeels, 1975; Minamikawa and Koshiba, 1979). Upon germination of the seeds, the storage proteins in the PSV are degraded by a papain-type proteinase, designated SH-EP (Mitsuhashi et al., 1986; Okamoto and Minamikawa, 1998) and the PSV is converted to a lytic vacuole (LV). Recently, it has been suggested that mass transport of proSH-EP from the endoplasmic reticulum (ER) to the PSV by ER-derived vesicles with a diameter of 200–500 nm mediates the characteristic/rapid conversion of PSV to LV in cotyledon cells (Toyooka et al., 2000). Although the degradation mechanism of storage proteins has been gradually resolved, the breakdown processes of another major storage material, starch, are still unclear. By biochemical analysis,  $\alpha$ -amylase was identified as the enzyme that has a major role in the degradation of stored starch in the cotyledons of germinated *V. mungo* seeds (Koshiba and Minamikawa, 1981), but it remains open how the enzyme reaches SG or how degradation of SG occurs in the cotyledon cells. Since  $\alpha$ -amylase has a signal peptide (Yamauchi et al., 1994) that should be recognized with signal recognition particles, the enzyme would enter the lumen of the ER (von Heijne, 1983) and thus is expected to be further transported to the vacuoles or secreted by the endomembrane system. This supposed intracellular localization of  $\alpha$ -amylase indicates that the enzyme is not directly sorted to SG originating from plastids.

In this study, we first identified the intracellular localization of  $\alpha$ -amylase in the cotyledon cells of *V. mungo* seedlings or embryo axis-removed (detached) seeds by immunocytochemical assays using affinity-purified anti- $\alpha$ -amylase antibody. The results obtained showing the vacuolar localization of  $\alpha$ -amylase in the cotyledon cells led us to observe the ultrastructures of the cotyledon cells to see the interaction of the vacuoles with the SG. The SG was wrapped with the acidic cell compartment that would be formed by fusion of a de novo synthesized acidic vesicle and subsequently incorporated into the LV. In addition, a distinct autophagic process to that for SG was found to be involved in the degradation of cytoplasm and mitochondrion. We showed that at least two distinct autophagic processes function for the degradation of the SG and other cytoplasmic components in the cells of the germinating cotyledon.

## Results

### Expression of $\alpha$ -amylase in attached or detached cotyledons

We have previously reported that removal of the embryonic axes from *V. mungo* seeds had effects on expression

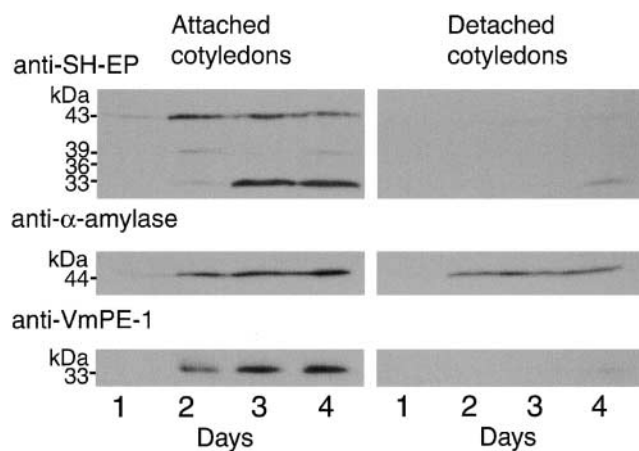


**Figure 1. Changes with time in amounts of SH-EP,  $\alpha$ -amylase, and VmPE-1 in cotyledons of *V. mungo* seedlings (Attached cotyledons) or embryo axis-removed cotyledons of *V. mungo* seeds (Detached cotyledons).** Attached or detached cotyledons were prepared as described in Materials and methods. 10 pairs of cotyledons were homogenized with 3 ml of 50 mM Tris-Cl (pH 7.4), and the homogenates were centrifuged at 15,000 g for 10 min. Supernatants (10  $\mu$ l each) were analyzed by SDS-PAGE immunoblotting with anti-SH-EP,  $\alpha$ -amylase, or VmPE-1 antibody.

of proteinase activity and degradation of storage reserves in cotyledons (Minamikawa, 1979; Yamauchi et al., 1994). When *V. mungo* seeds were allowed to germinate at 27°C in darkness, proteinase and amylase activities in the cotyledons (attached cotyledons) increased and reached a maximum level at 3 d after imbibition, and the amounts of storage proteins and starch gradually decreased during seed germination and subsequent seedling growth. When detached cotyledons (embryonic axes were removed from dry seeds) were prepared and incubated under the same conditions as above, mobilization of storage proteins and starch was not observed, and the proteinase activity remained at a low level. However, amylase activity appeared even in the detached cotyledons at an equivalent level to that in the attached cotyledons (Yamauchi et al., 1994). In this study, changes with time in amounts of a papain-type proteinase (SH-EP),  $\alpha$ -amylase and an asparaginyl endopeptidase (VmPE-1; Okamoto et al., 1994) in the attached or detached cotyledons were analyzed by SDS-PAGE and immunoblotting with anti-SH-EP,  $\alpha$ -amylase, or VmPE-1 antibody. In the attached cotyledons, these three hydrolases were synthesized de novo, and the amounts of these enzymes increased in *V. mungo* seeds within 4 d after imbibition (Fig. 1). In the detached cotyledons, expressions of SH-EP and VmPE-1 were markedly suppressed, but the expression level of  $\alpha$ -amylase was almost the same as that in the attached cotyledons (Fig. 1). These results indicate that  $\alpha$ -amylase is normally expressed even in detached cotyledon cells in which starch stored in SGs is intact (Minamikawa 1979; Yamauchi et al., 1994), and that  $\alpha$ -amylase is not directly transported to SGs but to other cell compartment(s) in the cotyledon cells. Thus, to determine the intracellular localization of the enzyme, subcellular fractionation and immunocytochemical assays of cotyledon cells were conducted.

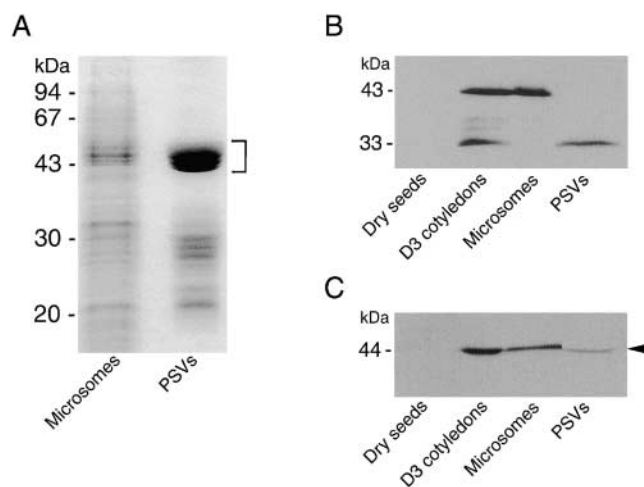


Figure 2. **Subcellular distribution of  $\alpha$ -amylase in *V. mungo* cotyledon cells.** Microsome and PSV fractions were prepared from cotyledons of day 3 seedlings as described in Materials and methods. Extracts from dry seeds and day 3 cotyledons, microsomes, and PSV fractions (20  $\mu$ g protein each) were separated by SDS-PAGE. Proteins in the gel were analyzed by Coomassie Brilliant blue staining (A), or by immunoblotting with anti-SH-EP antibody (B) or anti- $\alpha$ -amylase antibody (C). Bracket indicates the polypeptides derived from storage globulins. Arrowhead indicates  $\alpha$ -amylase.

### Intracellular localization of $\alpha$ -amylase in cotyledon cells

Cotyledon cells of day 3 dark-grown *V. mungo* seedlings were fractionated into microsome and PSV fractions, and both fractions were separated by SDS-PAGE. In the PSV fraction, polypeptides around 50 kD that were derived from storage globulins (Okamoto and Minamikawa, 1998) were enriched (Fig. 2 A). When the proteins in the gel were analyzed by immunoblotting with anti-SH-EP antibody, proSH-EP of 43-kD (ER and/or KDEL-tailed cysteine proteinase-accumulating vesicle [KV] form) and 33-kD mature SH-EP (vacuolar form) were detected in microsome and PSV fractions, respectively (Fig. 2 B; Okamoto et al., 1994). This suggests that fractionations of the microsome and PSV from cotyledon cells were successfully conducted. Probing the blots with anti- $\alpha$ -amylase antibody resulted in detection of  $\alpha$ -amylase with molecular mass of 44 kD in both the PSV and microsomal fractions (Fig. 2 C), suggesting that the enzyme is localized in PSV without proteolytic processing of the enzyme in PSV. By immunocytochemical analysis of the cotyledon cells with anti- $\alpha$ -amylase antibody, it was revealed that  $\alpha$ -amylase is localized in both PSVs and LVs (Fig. 3, A–F), which is possibly converted from the PSV by fusion of KV (Toyooka et al., 2000). Fig. 3 A shows that  $\alpha$ -amylase is localized in the PSV but not in the SG. Immunogold staining of the Golgi complex with anti- $\alpha$ -amylase antibody indicates that  $\alpha$ -amylase is transported to the PSV through a Golgi complex-dependent pathway (Fig. 3, B and C). When cotyledon cells were double immunogold-stained with anti- $\alpha$ -amylase polyclonal antibody and anti-SH-EP monoclonal antibody,  $\alpha$ -amylase and SH-EP were localized in the PSV and KV, respectively (Fig. 3 D), supporting the sorting of  $\alpha$ -amylase is Golgi complex dependent but not KV dependent. In addition to the PSV, the LV was densely

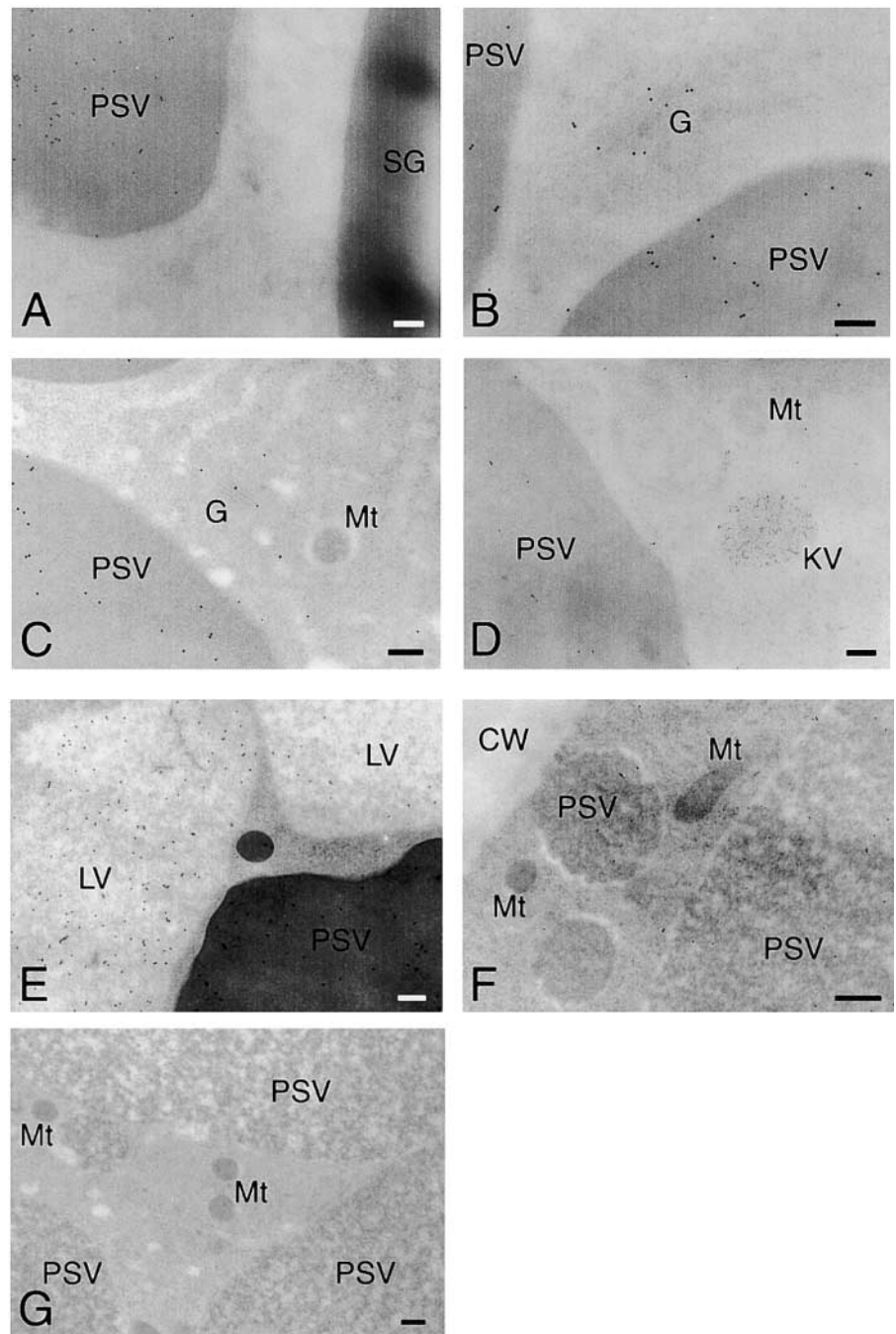
immunogold labeled (Fig. 3 E). This suggests that  $\alpha$ -amylase is transported to both the PSV and LV or sorted to the PSV before the conversion of PSVs to LVs occurs. When the detached cotyledons were incubated for 3 days and the cotyledon cells were analyzed with the same procedures, it was indicated that  $\alpha$ -amylase is transported to the PSV also in the detached cotyledons (Fig. 3, F and G).

### Breakdown of SG in LVs through autophagic process

Ultrastructural analyses of the cotyledon cells of normally germinated *V. mungo* seeds were conducted to observe how SG interacts with vacuoles to be degraded by  $\alpha$ -amylase. A cotyledon of a day 3 seedling is composed of heterologous cells with respect to the amount of reserves in the cells. Cells positioned near a vascular bundle (VB) were filled with storage materials (Fig. 4 A, region I), the reserves were degraded mostly in the cells far from the VB (Fig. 4 A, region III), and middle phase cells between filled cells and empty cells were observed (Fig. 4 A, region II). In the cells filled with reserves (filled cells), the border between the SG and cytoplasm was clear, and the electron density of the PSV was high since the storage proteins were intact (Fig. 4 B). The electron density of the PSV became low when the degradation of proteins started (Fig. 4 C). In the same cells, a membranous structure surrounding SGs was observed, and some regions with low electron density (LED) were found (Fig. 4 C). The LED area around the SG was enlarged in the empty cells in which most reserves were degraded and the PSV was converted to an LV (Fig. 4 D). In addition, vesicles with similar density to the LV and LED regions were observed in the empty cells (Fig. 4 E). These vesicles would be formed/synthesized de novo, since such vesicles were not found in the filled cells (Fig. 4 B). An SG surrounded with the LED region interacted with the LV (Fig. 4 E), and membrane fusion between the LED area around the SG and LV was observed (Fig. 4 F). The SG was found to be in the inside of the LV, and the shape of the SG was not round (Fig. 4 G), suggesting that degradation of SGs in LVs results in a change of shape of the SG. Fig. 4 H represents the immunogold image of degradation of an SG by  $\alpha$ -amylase in an LV. A major part of  $\alpha$ -amylase was found at the peripheral region of the SG, which was inserted into the LV (Fig. 4 H), suggesting the degradation of starch occurs at the peripheral area of SGs. In contrast to cells of attached cotyledons, conversion of PSVs to LVs was not observed, and SGs were not taken up into a PSV in the cells of detached cotyledons, which were incubated for 3 d (Fig. 4 I). In addition, neither the LED region around the SG nor the possibly de novo-synthesized vesicle with similar density to the LV was observed in the cells (Fig. 4 I). The degradation of the SG in LVs (Fig. 4, E–G) will indicate that the conversion of PSVs to LVs must occur before starch breakdown. By biochemical analyses for changes with time in amount of proteins and starch in the cotyledons of germinated *V. mungo* seeds, it has been revealed that the amount of proteins decreases in the cotyledons before starch breakdown (Minamikawa, 1979). The observation of degradation of the SG in LVs supports the previous report, since degradation of storage proteins in PSVs results in PSV conversion to LVs. Next, SGs, cells containing SGs, and thick sections were prepared from the cotyledons of day 3 seedlings and subsequently stained with LysoTracker red, an acidic or-



**Figure 3. Electron micrographs showing the immunogold localization of  $\alpha$ -amylase in attached cotyledons cells (A–E), detached cotyledons cells (F), or control for immunogold labeling (G).** (A) Anti- $\alpha$ -amylase antibody immunogold-stained PSV, but not SG. (B and C) Golgi complex and PSVs were both immunogold-labeled with anti- $\alpha$ -amylase antibody. (D) Immunogold localization of  $\alpha$ -amylase (15-nm particles) and SH-EP (10-nm particles).  $\alpha$ -Amylase and SH-EP were localized in PSVs and KVs, respectively. (E) Gold particles from anti- $\alpha$ -amylase antibody were detected in LVs as well as PSVs. (F) PSVs in detached cotyledons were immunogold labeled with anti- $\alpha$ -amylase antibody. (G) Immunogold staining of detached cotyledon cells without first antibody (anti- $\alpha$ -amylase antibody). No gold particles were observed in the cell. CW, cell wall; G, Golgi complex; KV, KDEL-tailed cysteine proteinase-accumulating vesicle; LV, lytic vacuole; Mt, mitochondrion; PSV, protein storage vacuole; SG, starch granule. Bars, 200 nm.



ganelle-selective probe. Small foci stained with the probe were found around the SG in broken cotyledon cells (Fig. 5, A–D) and in cells of cotyledon sections (Fig. 5, E–H). In addition, SGs were found to be wrapped with the acidic cell compartment (Fig. 5, I and J) and to be in the inside of a putative vacuole (Fig. 5, K and L). These LysoTracker red-stained small foci and cell compartments wrapping SGs explain the character of de novo-synthesized vesicles and the LED region around the SG, which were observed in the ultrastructural analyses of the cotyledon cells. The de novo-synthesized vesicles shown in Fig. 4 E may correspond to the small foci (Fig. 5, B, D, F, and H); and the LED region (Fig. 4, D and E), to the LysoTracker red-stained cell compartment wrapping SGs (Fig. 5 J). This also suggests the possibilities that vesicles or

small cell compartments with acidic pH fuse with SGs and that LED regions around SGs are built up by the fusion of such acidic vesicles/small cell compartments. When sections were prepared from detached cotyledons, which were incubated for 3 d and subsequently stained with the probe, no small foci were observed in the cells (Fig. 5, M–P). This is consistent with the result of ultrastructural observation, showing that neither de novo vesicle or LED region around SGs was detected in the cells of detached cotyledons (Fig. 4 I).

#### Autophagosome-mediated autophagy in cotyledon cells

In the course of the ultrastructural observation of the cotyledon cells, the autophagic process for cytoplasm and

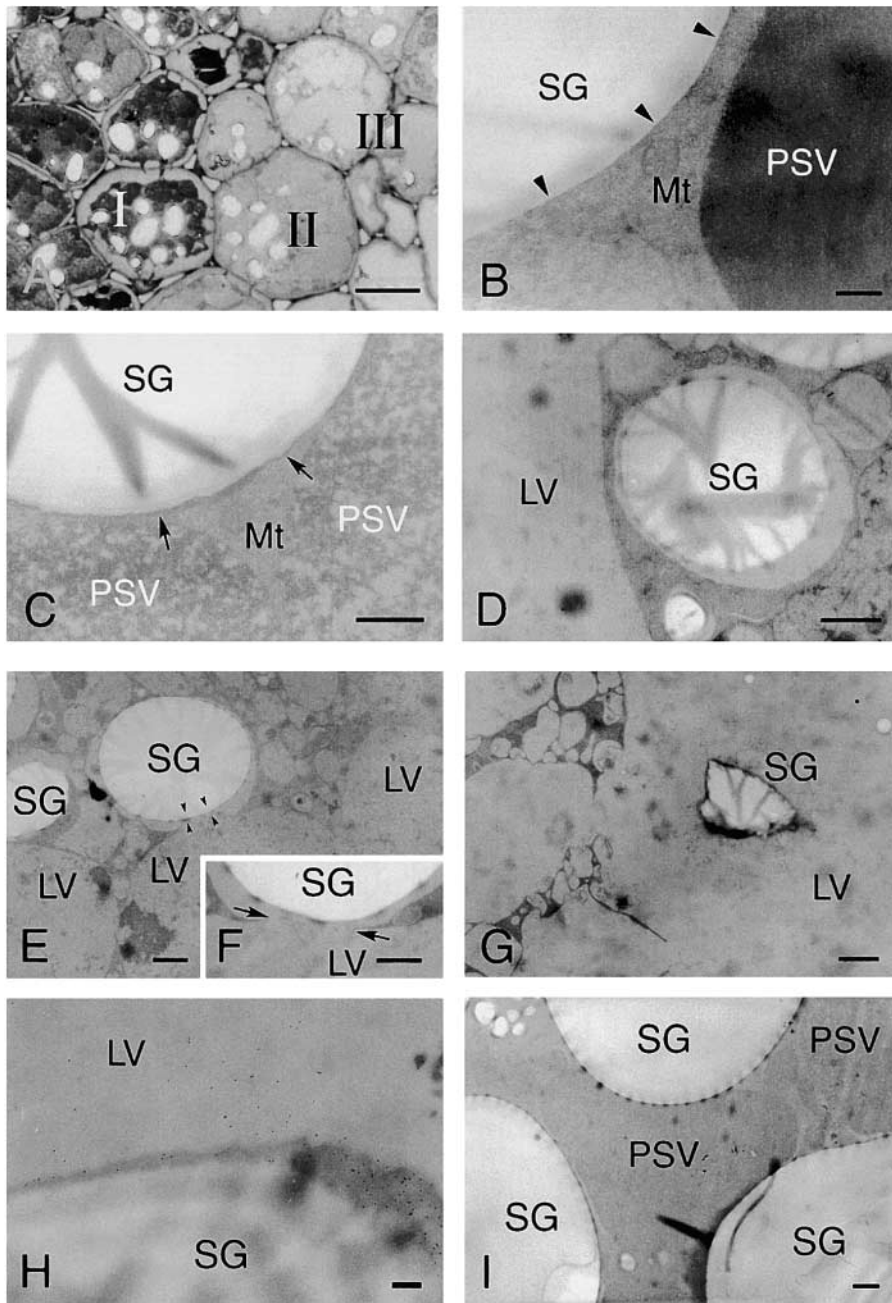


Figure 4. Electron micrographs showing ultrastructures of cotyledon cells of germinated *V. mungo* seeds (A–G), immunogold localization of  $\alpha$ -amylase in cotyledon cells (H), and ultrastructure of cells of detached cotyledons (I).

Toluidine blue (TB) staining of sections from cotyledons of day 3 *V. mungo* seedlings. Conversion from TB-stained cells (region I) to TB-stainless cells (region III) was accompanied with that of the PSV to LV. (B) SGs and PSVs in TB-stained cells (A, region I). The PSV was filled with storage proteins. Arrowheads indicate border between SGs and the cytoplasm. (C) SGs and PSVs in cotyledons at region II in A. Electron density of PSVs became low. SGs were surrounded with membranous structure (arrows). LED areas were found between SGs and the cytoplasm. (D) SG and LV in TB-stainless cells (region III in A). The PSV was converted to the LV in the cells. The areas around SG with LED were enlarged. (E) Ultrastructure of TB-stainless cells. SGs wrapped with a LED area contacted with LVs (arrowheads). Vesicles with similar density to LVs were observed. (F) LED membranes around the SGs fused with the LV membranes (arrow). (G) SGs were observed in LVs. The shape of SGs were largely different from those in B–E. (H) An immunogold image representing degradation of SGs by  $\alpha$ -amylase localized in LVs. Gold particles from anti- $\alpha$ -amylase antibody were densely detected in the peripheral region of SGs, which is inserted into the inside of the LV. (I) PSVs were not converted to LVs, and SGs were not taken up into PSVs in the cells of detached cotyledons. Neither low density areas around SGs nor vesicles with similar density to LV was observed in the cells. LV, lytic vacuole; Mt, mitochondrion; PSV, protein storage vacuole; SG, starch granule. Bars: (A) 50  $\mu$ m; (E and G) 2  $\mu$ m; (D, F, and I) 1  $\mu$ m; (B, C, and H) 200 nm.

mitochondrion, which is distinct from that for SGs, was detected. Two autophagosomes containing cytoplasm with a double membrane were observed in the attached cotyledon cells, and mitochondria and cytoplasm appeared to be enclosed with double-membranous structure similar to that of the endoplasmic reticulum (Fig. 6 A). Autophagosome containing mitochondria and cytoplasm was fused with the LV (Fig. 6 B), and an autophagic body containing mitochondria was observed in LVs (Fig. 6 C). These results are consistent with the reports that vacuoles in the cotyledon cells of *Vigna radiata* function as autophagic organelles (van der Wilden et al., 1980; Herman et al., 1981). When the detached cotyledons were incubated at 27°C in darkness for 3 d and then analyzed by conventional electron microscopy, as shown in Fig. 6, A–C, autophagosomes and autophagic bodies were observed in the detached cotyledon cells (Fig. 6, D and E),

although the conversion of PSV to LV did not occur (Figs. 4 I and 6, D and E). This indicates that autophagosome-mediated autophagy functions in detached cotyledons as well as attached cotyledons.

## Discussion

$\alpha$ -Amylase was transported to the vacuoles via the Golgi complex in the cotyledon cells of *V. mungo* seedlings. This is consistent with the postulated intracellular localization of the enzyme (Yamauchi et al., 1994). In cultured rice cells,  $\alpha$ -amylase was detected in the vacuoles and on cell walls, because  $\alpha$ -amylase genes exist as a multigene family and there are several kinds of  $\alpha$ -amylase in rice plant (Chen et al., 1994). In contrast,  $\alpha$ -amylase of *V. mungo* is encoded by a single gene (Yamauchi et al., 1994), explaining the observa-



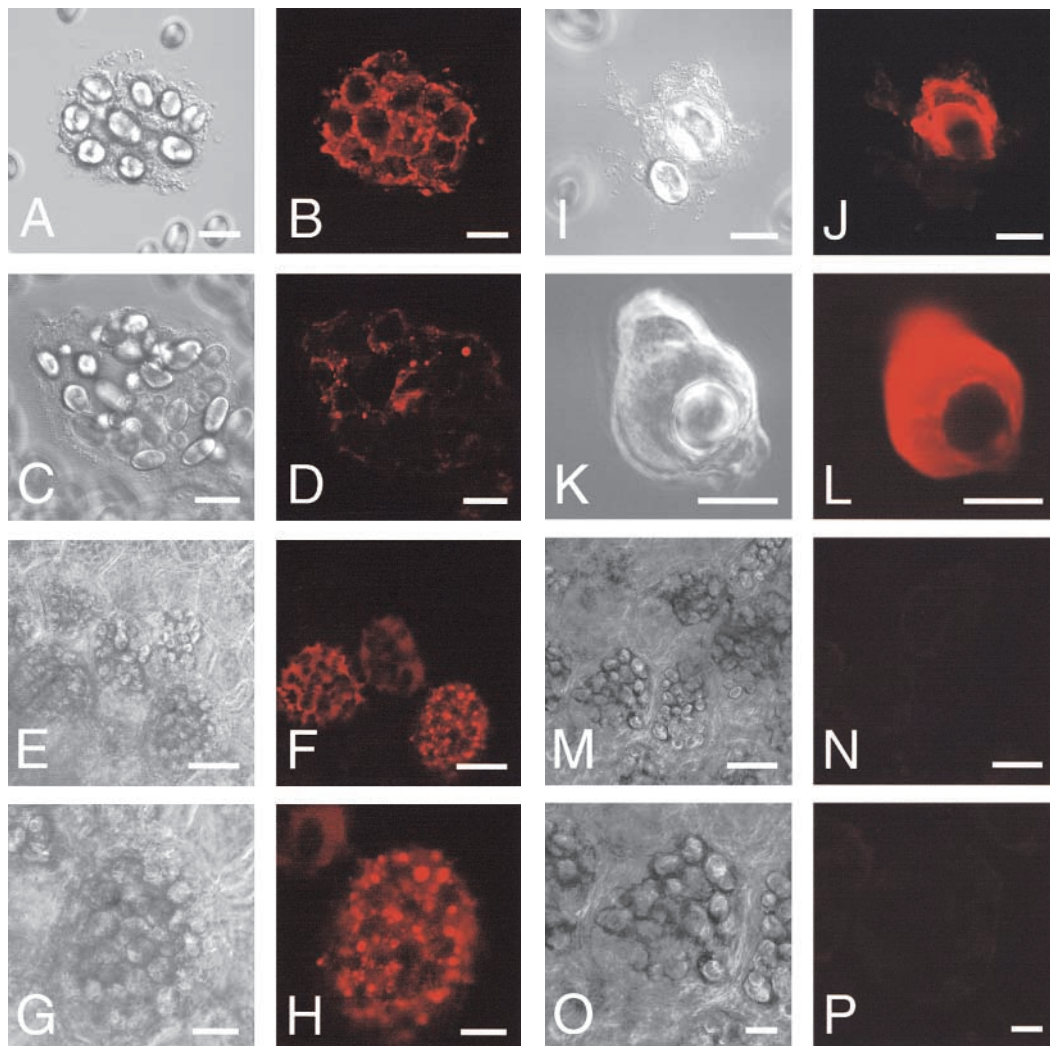


**Figure 5. LysoTracker red staining of partially broken cotyledon cells, SGs, or cotyledon sections.** Cotyledon cells, SGs, and sections were prepared from day 3 attached or detached cotyledons and stained with LysoTracker red as described in Materials and methods. (A) Differential interface-contrast image of a broken cell. (B) Fluorescent image of A. (C) Differential interface-contrast image of a broken cell. (D) Fluorescent image of C. (E) Differential interface-contrast image of cells of a section from attached cotyledons. (F) Fluorescent image of E. (G) Magnified image of E. (H) Magnified image of F. (I) Differential interface-contrast image of an SG. (J) Fluorescent image of I. (K) Differential interface-contrast image of an SG. (L) Fluorescent image of K. (M) Differential interface-contrast image of cells of a section from detached cotyledons. (N) Fluorescent image of M. (O) Magnified image of M. (P) Magnified image of O. Bars: (A–D, G–L, O, and P) 20  $\mu\text{m}$ ; (E, F, M, and N) 50  $\mu\text{m}$ .

tion of clear localization of  $\alpha$ -amylase only in the vacuoles of the cotyledon cells. The vacuolar sorting signals that have been identified (Chrispeels and Raikhel, 1992; Nakamura and Matsuoka, 1993) were not found in the amino acid sequence deduced from cDNA for  $\alpha$ -amylase, indicating the possibility of the existence of an unidentified vacuolar targeting signal on the amino acid sequence of  $\alpha$ -amylase of *V. mungo*.

Autophagic mechanisms have been intensively investigated in yeast, and at least two main autophagic machineries have been identified. First is macroautophagy: cytoplasm and/or mitochondria are sequestered into autophagosomes wrapped with a double membrane, and then the autophagosome fuses with vacuoles (Takeshige et al., 1992; Baba et al., 1994). Second is microautophagy, which was identified in the degradation process of the peroxisome in glucose-treated yeast cells. This autophagic process is preceded by engulf-

ment of the peroxisome by vacuoles and is called micropexophagy (Tuttle and Dunn, 1995; Sakai et al., 1998). Investigations for autophagy in plants have been mainly conducted with cultured cells, since removal of nutrients in culture medium often induces autophagy in the cultured cells (Chen et al., 1994; Aubert et al., 1996; Moriyasu and Ohsumi, 1996). Therefore, the study of autophagy related to plant development/senescence has been limited. This study indicates that two distinct autophagic processes function in the cotyledon cells of *V. mungo* seedlings for the degradation of reserves and cellular components. A model of two types of autophagies in a cotyledon cell is presented in Fig. 7. One autophagic process is the degradation of SGs. In the cotyledon cells, the SG is wrapped with an acidic compartment that is possibly built up by the fusion of small acidic vesicle synthesized de novo and subsequently incorporated into the LV that is converted from PSV by the fusion of KV.

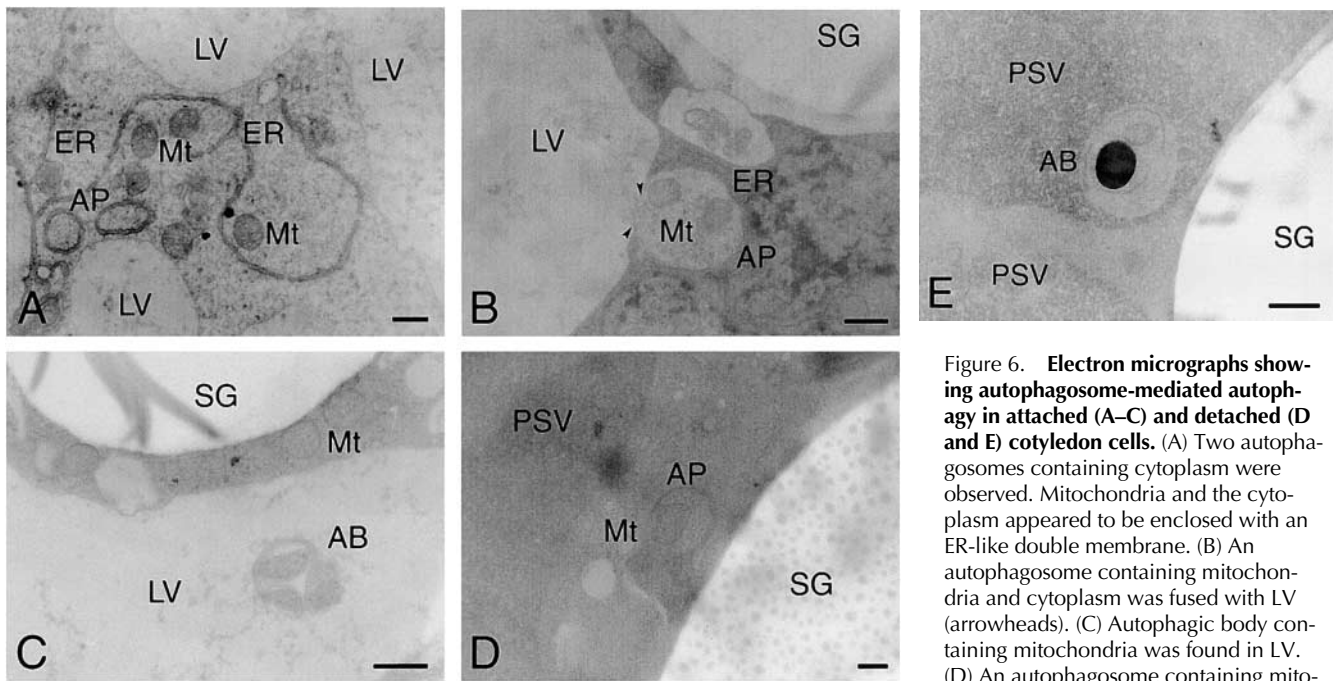


Figure 6. **Electron micrographs showing autophagosome-mediated autophagy in attached (A–C) and detached (D and E) cotyledon cells.** (A) Two autophagosomes containing cytoplasm were observed. Mitochondria and the cytoplasm appeared to be enclosed with an ER-like double membrane. (B) An autophagosome containing mitochondria and cytoplasm was fused with LV (arrowheads). (C) Autophagic body containing mitochondria was found in LV. (D) An autophagosome containing mitochondria and cytoplasm was observed.

The PSV was not converted into the LV. (E) Autophagic body was observed in the PSV of detached cotyledon cells. AB, autophagic body; AP, autophagosome; ER, endoplasmic reticulum; LV, lytic vacuole; Mt, mitochondrion; PSV, protein storage vacuole; SG, starch granule. Bars, 200 nm.

As for de novo-synthesized vesicles with acidic pH, it is known that small vacuoles are synthesized de novo in the aleurone cells of germinated barley grains (Paris et al., 1996; Swanson et al., 1998; Sansebastiano et al., 2001). The vesicles in the cotyledon cells may correspond to the newly synthesized vacuoles. The degradation of SG in LV was observed by ultrastructural and immunocytochemical analyses of the cotyledon cells. However, we could not clearly identify how wrapped SGs were inserted into the inside of vacuoles. Two possibilities were suggested for the cellular mechanism of the insertion of SGs into LVs. A wrapped SG is further surrounded by several LVs and finally incorporated into the LV through membrane fusion between LVs (Fig. 4 E), or the membrane of the LED region around the SG is fused to that of the LV (Fig. 4 F), resulting in the insertion of SGs into the inside of LVs. It cannot be excluded that both mechanisms function synergistically for effective vacuolar degradation of LED-wrapped SGs. In yeast cells, the peroxisome is wrapped with thin or fragmented vacuoles at the first step of micropexophagy, and subsequently the wrapped peroxisome is engulfed into the vacuole (Tuttle and Dunn, 1995; Sakai et al., 1998). Degradation of SGs may be proceeded by a mechanism analogous to micropexophagy, since SG was also wrapped with acidic cell compartments.

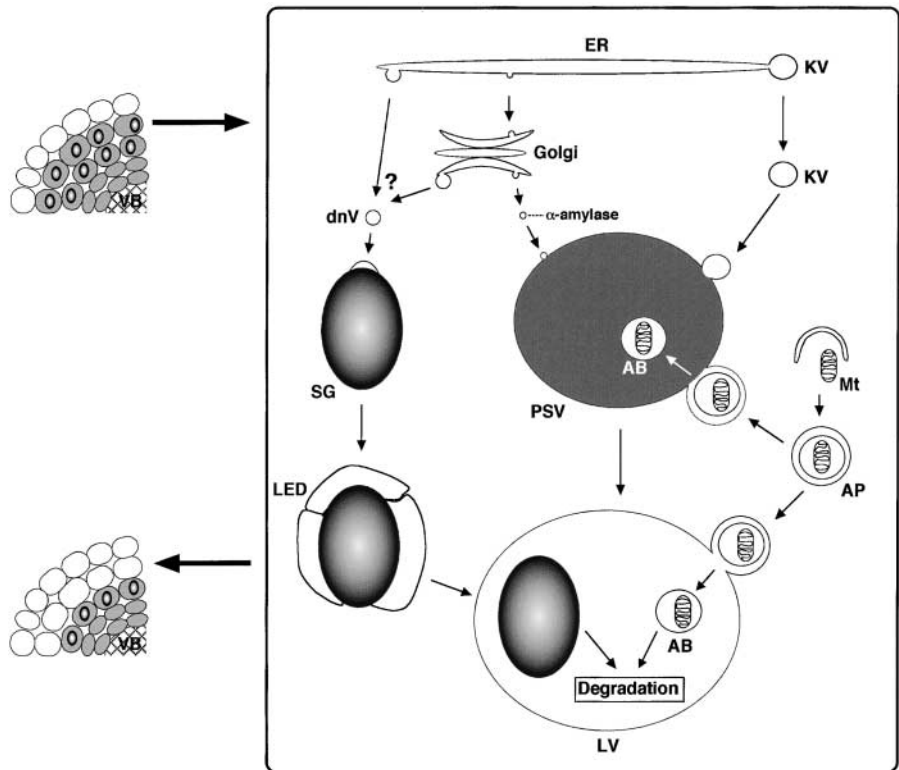
The other autophagic machinery in the cotyledon cells is the macroautophagy that is mediated by autophagosome. In the autophagosome, mitochondria and cytoplasm were observed (Fig. 6, A–E), which corresponded to autophagic vesicles reported in the cotyledons of *V. radiata* (van der Wilden et al., 1980). These findings suggest that the cytoplasm and mitochondria in the cotyledon cells are sorted to the vacuoles via the autophagosome in a similar manner to those in yeast cells (Takeshige et al., 1992; Baba et al.,

1994). The macroautophagy was detected in both the attached and detached cotyledon cells, but the autophagic process for the degradation of SGs was observed only in the attached cotyledon cells. In the detached cotyledons, SH-EP was barely expressed, and storage proteins remained intact, resulting in no conversion of PSVs to LVs and in loss of SG degradation in LVs (Fig. 7).

The autophagic programmed cell death (PCD) detected in the cotyledon cells is different from PCD by hypersensitive response, the plant defence system against pathogens, or by differentiation of tracheary elements. PCD induced by hypersensitive response is highly similar to apoptosis (Goodman and Novacky, 1996), and that of the differentiation of tracheary elements is induced by tonoplast disruption and subsequent release of vacuolar hydrolases into the cytosol (Fukuda, 1997). Higher plants use the autophagic PCD for senescing organs rather than the apoptotic or hydrolase-releasing PCD, since hydrolysis of cellular materials in vacuoles does not damage the senescing cells, and withdrawal of cellular materials from the cells can be successfully achieved (Jones, 2000). In fact, two kinds of autophagic processes, micropexophagy-like and autophagosome-mediated autophagies, were found to function in the germinated cotyledon cells, and a possible relationship between senescence and autophagy was indicated. Moreover, the ultrastructural analysis of senescing leaves also indicated that the autophagic PCD occurs in the senescing leaves of kidney beans (Minamikawa et al., 2001). Plants use vacuoles for storage of materials as well as hydrolysis of needless cellular components (for review see Herman and Larkins, 1999). In addition to these well-known functions of vacuoles, the autophagic vacuoles in senescing cells may be one way of the flexible uses of vacuoles by plants, since the turnover and re-

**Figure 7. A model of autophagic processes in the cotyledon cell of germinated *V. mungo* seeds.**

The digestion of storage proteins in germinated cotyledons occurs in cells farthest from the VB. The proform of SH-EP synthesized in the lumen of the ER is packed into the KV at the edge or the middle region of the ER. The KV filled with proSH-EP buds off from the ER, bypasses the Golgi complex, and fuses with the PSV, resulting in the release of proSH-EP into the inside of the PSV. This mass transport of proteinase triggers the breakdown of storage proteins and conversion of the PSV into the LV.  $\alpha$ -Amylase is transported to the PSV via the Golgi complex. The acidic vesicle is synthesized *de novo* (dnV) and fuses with the SG. The transport pathway of dnV to the SG remains open. The possibility that dnVs are derived from the LV by a process of fragmentation of LVs cannot be excluded. An LED area is formed around the SG by fusion of dnVs, and an SG wrapped with LED area is incorporated into the LV by membrane fusion between the LED area around SGs and LVs or engulfment of SGs by LVs. Autophagosome carries mitochondria and cytoplasm to the PSV and/or LV.



SGs, mitochondria, and cytoplasm are degraded by hydrolases in LVs. These autophagic processes mediate the change of the cotyledon cells filled with storage materials (shaded cells) into cells in that most cell components are degraded (nonshaded cells). In detached cotyledons, SH-EP is only slightly expressed, and the KV is not formed, resulting in loss of conversion of the PSV to the LV. The acidic vesicle (dnV) is not synthesized in the detached cotyledon cells. AB, autophagic body; AP, autophagosome; dnV, *de novo*-synthesized acidic vesicle; ER, endoplasmic reticulum; KV, KDEL-tailed cysteine proteinase-accumulating vesicle; LED, low electron density; LV, lytic vacuole; Mt, mitochondrion; PSV, protein storage vacuole; VB, vascular bundle.

capture of cellular materials are exclusively developed in plants.

## Materials and methods

### Plant materials

*V. mungo* seeds were germinated on layers of wet filter paper at 27°C in darkness, and the cotyledons were collected on days 1 to 4 after imbibition. The cotyledons from the seedlings were used as attached cotyledons. To prepare detached cotyledons, embryo axes were removed from dry *V. mungo* seeds, and the embryo axis-removed cotyledons were incubated on wet filter paper at 27°C in darkness for 1–4 d.

### Gel electrophoresis and immunoblotting

SDS-PAGE and immunoblotting were performed as described previously (Mitsubishi and Minamikawa, 1989).

### Preparation of antibodies

$\alpha$ -amylase was purified according to Koshiba and Minamikawa (1981), and the purified enzyme (3 mg) was immobilized to 3 ml of ECH-Sepharose 4B (Amersham Pharmacia Biotech) according to the manufacturer's instructions. 25 ml of antiserum to  $\alpha$ -amylase was precipitated by the addition of 12.5 ml of saturated ammonium sulfate solution, and the precipitate was dialyzed against PBS. After centrifugation of the dialyzed solution, the supernatant was applied to the column of the  $\alpha$ -amylase-immobilized Sepharose, which had been equilibrated with PBS. The column was washed first with PBS and further with 0.5 M NaCl in PBS. The antibody bound to the column was eluted by 0.1 M glycine-HCl (pH 2.5) containing 0.5 M NaCl, and the eluate was immediately neutralized with 1 M Tris-Cl (pH 8.0). The antibody obtained from the column was dialyzed

against PBS containing 0.1% sodium azide and used as anti- $\alpha$ -amylase antibody. Monoclonal and polyclonal antibodies against SH-EP (Toyooka et al., 2000) and anti-VmPE-1 antibody (Okamoto and Minamikawa, 1999) were prepared as described previously.

### Immunocytochemistry and ultrastructural analysis

Cotyledons of 3-d-grown *V. mungo* seedlings or detached cotyledons incubated for 3 d were cut into  $\sim 1$ -mm<sup>3</sup> cubes and fixed with 4% paraformaldehyde and 2% glutaraldehyde in 0.1 M potassium phosphate buffer (pH 7.4) for 4 h at 4°C. After fixation of the tissue pieces, they were dehydrated in a graded methanol series. Procedures for ultrastructural analysis were conducted as described previously (Hara-Nishimura et al., 1993). For immunocytochemical analysis, the dehydrated pieces were embedded in a hard formulation of LR White resin. Ultrathin sections mounted on nickel grids (600 mesh; Electron Microscopy Sciences) were blocked with 10% fetal bovine serum in TBS (25 mM Tris-Cl, pH 7.4, 150 mM NaCl) for 10 min at room temperature. The sections were then labeled with affinity-purified antibody to  $\alpha$ -amylase (diluted 1:1) or SH-EP (1:1) in TBS. After being washed with TBS, the sections were indirectly labeled with colloidal gold particles coupled to goat anti-rabbit IgG or colloidal gold particles coupled to goat anti-mouse IgG. The gold-labeled sections were then washed with TBS, rinsed in water, and stained with 4% aqueous uranyl acetate. The grids were examined and photographed with a transmission electron microscope (model 1010EX; JEOL) at 80 kV.

### Subcellular fractionation of cotyledon cells, sectioning of cotyledons, and confocal laser scanning microscope

The microsome and PSV fractions were obtained from the cotyledons of day 3 *V. mungo* seedlings as described (Okamoto et al., 1994). To prepare the fraction containing SGs and partially broken cotyledon cells containing SGs, 50 pairs of day 3 cotyledons were gently ground in a mortar and pestle with 5 ml of 50 mM Hepes-KOH (pH 7.5) containing 0.5 M sucrose, 5



mM MgCl<sub>2</sub>, 1 mM EDTA. The homogenate was filtered through a nylon mesh (150 µm in diameter), and the filtrate was allowed to stand for 10 min on ice for precipitation of SGs and broken cells containing SGs. The precipitate was resuspended in 5 ml of homogenization buffer, and the resuspension was again allowed to stand for 10 min on ice. After the precipitate was resuspended with the buffer, LysoTracker red DND-99 (Molecular Probes) was added at the final concentration of 1 µM. After incubation for 15 min and subsequent washing twice, the samples were observed by confocal laser scanning microscopy (LSM 510, ZEISS) using a 543-nm Helium-Neon laser for excitation and a 560-nm-long pass filter for the detection of fluorescence. Cotyledons from day 3 seedlings or detached cotyledons incubated for 3 d were transversally sliced by a razor blade into ~0.5-mm-thick portions in the buffer (50 mM Hepes-KOH, pH 7.5, 0.5 M sucrose, 5 mM MgCl<sub>2</sub>, 1 mM EDTA). The sections were washed with the buffer and subsequently incubated in the buffer containing 1 µM LysoTracker red DND-99 for 10 min. After washing the sections three times, the samples were observed by confocal laser scanning microscopy as described above.

We thank Dr. Yoshinori Ohsumi, Dr. Kenji Noda, and Mr. Hideki Hanaoka for their critical reading of the manuscript and useful discussions and suggestions. We are grateful to Dr. Teruo Kirikae for his assistance on conducting laser scanning microscopic observations.

This work was supported in part by Grants-in-Aid for Scientific Research (12740441) from the Ministry of Education, Science and Culture of Japan.

Submitted: 21 May 2001

Revised: 5 July 2001

Accepted: 16 July 2001

## References

- Akazawa, T., and I. Hara-Nishimura. 1985. Topographic aspects of biosynthesis, extracellular secretion, and intracellular storage of proteins in plant cells. *Plant Mol. Biol.* 36:441–472.
- Aubert, S., E. Gout, R. Bligny, D. Marty-Mazars, F. Barrieu, J. Alabouvette, F. Marty, and R. Douce. 1996. Ultrastructural and biochemical characterization of autophagy in higher plant cells subjected to carbon deprivation: control by the supply of mitochondria with respiratory substrates. *J. Cell Biol.* 133:1251–1263.
- Baba, M., K. Takeshige, N. Baba, and Y. Ohsumi. 1994. Ultrastructural analysis of the autophagic process in yeast: detection of autophagosomes and their autophago-somes characterization. *J. Cell Biol.* 124:903–913.
- Baulcombe, D.C., and D. Buffard. 1983. Gibberellic acid-regulated expression of α-amylase and six other genes in wheat aleurone layers. *Planta.* 157:493–501.
- Bewley, J.D., and M. Black. 1978. *Physiology and Biochemistry of Seeds.* Springer-Verlag, Berlin, Heidelberg, and New York. 229–241.
- Bewley, J.D., and M. Black. 1994. *Seeds: Physiology of Development and Germination.* 2nd ed. Plenum Press, New York and London. 1–31.
- Chen, M.-H., L.-F. Liu, Y.-R. Chen., H.-K. Wu, and S.-M. Yu. 1994. Expression of α-amylase, carbohydrate metabolism, and autophagy in cultured rice cells is coordinately regulated by sugar nutrient. *Plant J.* 6:625–636.
- Chrispeels, M.J., and N.V. Raikhel. 1992. Short peptide domains target proteins to plant vacuoles. *Cell.* 68:613–618.
- Fincher, G.B. 1989. Molecular and cellular biology associated with endosperm mobilization in germinating cereal grains. *Plant Mol. Biol.* 40:305–346.
- Fukuda, H. 1997. Traceary element differentiation. *Plant Cell.* 9:1147–1156.
- Goodman, R.N., and A.J. Novacky. 1996. *The Hypersensitive Reaction in Plants to Pathogens: A Resistance Phenomenon.* 2nd ed. American Phytopathology Society. St. Paul, MN. 256 pp.
- Greenberg, J.T. 1996. Programmed cell death: a way of life for plants. *Proc. Natl. Acad. Sci. USA.* 93:12094–12097.
- Hara-Nishimura, I., I. Takeuchi, K. Inoue and M. Nishimura. 1993. Vesicle transport and processing of the precursor to 2S albumin in pumpkin. *Plant J.* 4:793–800.
- Harris, N., and M.J. Chrispeels. 1975. Histochemical and biochemical observations on storage protein metabolism and protein body autolysis in cotyledons of germinating mung beans. *Plant Physiol.* 56:292–299.
- Herman, E.M., B. Baumgartner, and M.J. Chrispeels. 1981. Uptake and apparent digestion of cytoplasmic organelles by protein bodies (protein storage vacuoles) in mung bean cotyledons. *Eur. J. Cell Biol.* 24:226–235.
- Herman, E.M., and B.A. Larkins. 1999. Protein storage bodies and vacuoles. *Plant Cell.* 11:601–613.
- Jacobsen, J.V., and L.R. Beach. 1985. Control of transcription of α-amylase and rRNA genes in barley aleurone protoplasts by gibberellin and abscisic acid. *Nature.* 316:275–277.
- Jones, A. 2000. Does the plant mitochondrion integrate cellular stress and regulate programmed cell death? *Trends Plant Sci.* 5:225–230.
- Koehler, S.M., and T.-H.D. Ho. 1990. Hormonal regulation, processing, and secretion of cysteine proteinases in barley aleurone layers. *Plant Cell.* 2:769–783.
- Koshiba, T., and T. Minamikawa. 1981. Purification by affinity chromatography of α-amylase a main amylase in cotyledons of *Vigna mungo* seeds. *Plant Cell Physiol.* 22:979–987.
- Minamikawa, T. 1979. Hydrolytic enzyme activities and degradation of storage components in cotyledons of germinating *Phaseolus mungo* seeds. *Bot. Mag. Tokyo.* 92:1–12.
- Minamikawa, T., and T. Koshiba. 1979. Histochemical studies on mobilization of storage components in cotyledons of germinating *Phaseolus mungo* seeds. *Bot. Mag. Tokyo.* 92:325–332.
- Minamikawa, T., K. Toyooka, T. Okamoto, I. Hara-Nishimura. 2001. Degradation of ribulose 1,5-biphosphate carboxylase/oxygenase by vascular enzymes of senescing French bean leaves: immunocytochemical and ultrastructural observations. *Protoplasma.* In press.
- Mitsuhashi, W., T. Koshiba, and T. Minamikawa. 1986. Separation and characterization of two endopeptidases from cotyledons of germinating *Vigna mungo* seeds. *Plant Physiol.* 80:628–634.
- Mitsuhashi, W., and T. Minamikawa. 1989. Synthesis and posttranslational activation of sulfhydryl-endopeptidase in cotyledons of germinating *Vigna mungo* seeds. *Plant Physiol.* 89:274–279.
- Moriyasu, Y., and Y. Ohsumi. 1996. Autophagy in tobacco suspension-cultured cells in response to sucrose starvation. *Plant Physiol.* 111:1233–1241.
- Nakamura, K., and K. Matsuoka. 1993. Protein targeting to the vacuole in plant cells. *Plant Physiol.* 101:1–5.
- Ness, P.J., and H.W. Woolhouse. 1980. RNA synthesis in *Phaseolus* chloroplasts. *J. Exp. Bot.* 31:235–245.
- Nooden, L.D. 1988. The phenomenon of senescence and aging. In *Senescence and Aging in Plants.* L.D. Nooden and A.C. Leopold, editors. Academic Press, San Diego, CA. 1–50.
- Okamoto, T., H. Nakayama, K. Seta, T. Isobe, and T. Minamikawa. 1994. Post-translational processing of a carboxy-terminal propeptide containing a KDEL sequence of plant vacuolar cysteine endopeptidase (SH-EP). *FEBS Lett.* 351:31–34.
- Okamoto, T., and T. Minamikawa. 1998. A vacuolar cysteine endopeptidase (SH-EP) that digests seed storage globulin: characterization, regulation of gene expression, and posttranslational processing. *J. Plant Physiol.* 152:675–682.
- Okamoto, T., and T. Minamikawa. 1999. Molecular cloning and characterization of *Vigna mungo* processing enzyme 1 (VmPE-1), an asparaginyl endopeptidase possibly involved in posttranslational processing of a vacuolar cysteine endopeptidase (SH-EP). *Plant Mol. Biol.* 39:63–73.
- Paris, N., C.M. Stanley, R.L. Jones, and J.C. Rogers. 1996. Plant cells contain two functionally distinct vacuolar compartments. *Cell.* 85:563–572.
- Pennell, R.I., and C. Lamb. 1997. Programmed cell death in plants. *Plant Cell.* 9:1157–1168.
- Russell, S.D. 1992. Double fertilization. *Int. Rev. Cytol.* 140:357–390.
- Sakai, Y., A. Koller, L.K. Rangell, G.A. Keller, and S. Subramani. 1998. Peroxisome degradation by microautophagy in *Pichia pastoris*: identification of specific steps and morphological intermediates. *J. Cell Biol.* 141:625–636.
- Sansebastiano, G.P., N. Paris, S. Marc-Martin, and J.M. Neuhaus. 2001. Regeneration of a lytic central vacuole and of neutral peripheral vacuoles can be visualized by green fluorescent proteins targeted to either type of vacuoles. *Plant Physiol.* 126:78–86.
- Shintani, A., H. Kato, and T. Minamikawa. 1997. Hormonal regulation of expression of two cysteine endopeptidase genes in rice seedlings. *Plant Cell Physiol.* 38:1242–1248.
- Sutoh, K., H. Kato, and T. Minamikawa. 1999. Identification and possible roles of three types of endopeptidase from germinated wheat seeds. *J. Biochem.* 126: 700–707.
- Swanson, S.J., P.C. Bethke, and R.L. Jones. 1998. Barley aleurone cells contain two types of vacuoles: characterization of lytic organelles by use of fluorescent probes. *Plant Cell.* 10:685–698.
- Takeshige, K., M. Baba, S. Tsuboi, T. Noda, and Y. Ohsumi. 1992. Autophagy in yeast demonstrated with proteinase-deficient mutants and conditions for its induction. *J. Cell Biol.* 119:301–311.

- Toyooka, K., T. Okamoto, and T. Minamikawa. 2000. Mass transport of a pro-form of a KDEL-tailed cysteine proteinase (SH-EP) to protein storage vacuoles by endoplasmic reticulum-derived vesicle is involved in protein mobilization in germinating seeds. *J. Cell Biol.* 148:453–463.
- Tuttle, D.L., and W.A. Dunn, Jr. 1995. Divergent modes of autophagy in the methylotrophic yeast *Pichia pastoris*. *J. Cell Sci.* 108:25–35.
- van der Wilden, W., E.M. Herman, and M.J. Chrispeels. 1980. Protein bodies of mung bean cotyledons as autophagic organelles. *Proc. Natl. Acad. Sci. USA.* 77:428–432.
- von Heijne, G. 1983. Patterns of amino acids near signal-sequence cleavage site. *Eur. J. Biochem.* 133:17–21.
- Yamauchi, D., H. Takeuchi, and T. Minamikawa. 1994. Structure and expression of  $\alpha$ -amylase gene from *Vigna mungo*. *Plant Cell Physiol.* 35:705–711.
- Young, T.E., D.R. Gallie, and D.A. DeManson. 1997. Ethylene-mediated programmed cell death during maize endosperm development of wild-type and shrunken2 genotypes. *Plant Physiol.* 115:737–751.